Tyrosyl-tRNA synthetase stimulates thrombopoietin-independent hematopoiesis accelerating recovery from thrombocytopenia

Taisuke Kanaji[a,b,1], My-Nuong Vo[a,c,1], Sachiko Kanaji[a,b,c,1], Alessandro Zarpellon[a,b], Ryan Shapiro[a,c], Yosuke Morodomi[a,b], Akinori Yuzuriha[d], Koji Eto[d], Rajesh Belani[a,c], Minh-Ha Do[e,2], Xiang-Lei Yang[a,c], Zaverio M. Ruggeri[a,b,3], and Paul Schimmel[a,c,f,3]

[a]Department of Molecular Medicine, The Scripps Research Institute, La Jolla, CA 92037; [b]MERU-Roon Research Center on Vascular Biology and Thrombosis, The Scripps Research Institute, La Jolla, CA 92037; [c]The Scripps Laboratories for tRNA Synthetase Research, The Scripps Research Institute, La Jolla, CA 92037; [d]Department of Clinical Application Research, Center for iPS Cell Research and Application, Kyoto University, 606-8507 Kyoto, Japan; [e]aTyr Pharma, San Diego, CA 92121; and [f]Department of Molecular Medicine, The Scripps Research Institute, Jupiter, FL 33458

Contributed by Paul Schimmel, July 12, 2018 (sent for review April 25, 2018; reviewed by Michael Ibba and Andrew Weyrich)

New mechanisms behind blood cell formation continue to be uncovered, with therapeutic approaches for hematological diseases being of great interest. Here we report an enzyme in protein synthesis, known for cell-based activities beyond translation, is a factor inducing megakaryocyte-biased hematopoiesis, most likely under stress conditions. We show an activated form of tyrosyl-tRNA synthetase (YRS^{ACT}), prepared either by rationally designed mutagenesis or alternative splicing, induces expansion of a previously unrecognized high-ploidy Sca-1^+ megakaryocyte population capable of accelerating platelet replenishment after depletion. Moreover, YRS^{ACT} targets monocytic cells to induce secretion of transacting cytokines that enhance megakaryocyte expansion stimulating the Toll-like receptor/MyD88 pathway. Platelet replenishment by YRS^{ACT} is independent of thrombopoietin (TPO), as evidenced by expansion of the megakaryocytes from induced pluripotent stem cell-derived hematopoietic stem cells from a patient deficient in TPO signaling. We suggest megakaryocyte-biased hematopoiesis induced by YRS^{ACT} offers new approaches for treating thrombocytopenia, boosting yields from cell-culture production of platelet concentrates for transfusion, and bridging therapy for hematopoietic stem cell transplantation.

tyrosyl-tRNA synthetase | megakaryopoiesis | thrombocytopenia

During evolution, aminoacyl-tRNA synthetases (aaRSs) acquired a wide variety of nontranslational functions in pathways controlling inflammation, angiogenesis, oncogenesis, and apoptosis (1–4). These ex-translational functions are associated with novel domains or sequence elements appended to or inserted into the core tRNA synthetase architecture. Once a new domain was added in evolution, it was retained thereafter as the tree of life was ascended. In this way, the overall architecture of a tRNA synthetase increased in complexity as evolution proceeded. This observation suggests strong selective pressure to retain the added structural complexity. Interestingly, over 200 splice variants have been annotated for human tRNA synthetases, and the majority of these ablate or disrupt the catalytic domain but retain the noncatalytic elements (5). These ablations and retentions clearly point to a repurposing of the synthetase in a way that supports retention of repurposed functions.

In addition to regulatory roles in the cytoplasm (6–8), ex-translational activities of tRNA synthetases are often associated with nuclear and extracellular functions (9–15). These functions depend on specific receptor interaction or protein–partner interactions, such as VE cadherin, PARP-1, Nrp1, and TRIM28 (9, 12, 16, 17). As an example of interest here, human tyrosyl-tRNA synthetase (YRS) can be split by splicing or natural proteolysis into two fragments with distinct novel activities (18, 19). These activities are masked in the native, full-length protein, which is composed of a Rossmann fold catalytic unit, anticodon-recognition domain, and endothelial monocyte-activating polypeptide II (EMAPII)-homologous C-terminal domain (Fig. 1*A*) (20). These nontranslational activities depend on two motifs that were acquired in evolution. One is a critical ELR tripeptide motif that was inserted into the catalytic domain at the stage of insects. The EMAPII domain is an appended domain (dispensable for aminoacylation) that was added at the time of appearance of fungal organisms and later incorporated a critical motif (for cell signaling) at the stage of insects. After their acquisition, both of these motifs were retained thereafter as the tree of life expanded (21). Leukocyte elastase cleaves secreted YRS into the N-terminal catalytic unit and anticodon-binding domain as one unit, and the EMAPII domain as a separate fragment. Thus, fragmentation exposes the motifs needed for cytokine activities that are masked in native YRS by a tether between N- and C-terminal regions. High-resolution X-ray structures of each fragment

Significance

Aminoacyl-tRNA synthetases (aaRSs) catalyze aminoacylation of tRNAs in the first step of protein synthesis in the cytoplasm. However, in higher eukaryotes, they acquired additional functions beyond translation. In the present study, we show that an activated form of tyrosyl-tRNA synthetase (YRS^{ACT}) functions to enhance megakaryopoiesis and platelet production in vitro and in vivo. These findings were confirmed with human megakaryocytes differentiated from peripheral blood $CD34^+$ hematopoietic stem cells and with human induced pluripotent stem (iPS) cells. The activity of YRS^{ACT} is independent of thrombopoietin (TPO), as evidenced by expansion of the megakaryocytes from iPS cell-derived hematopoietic stem cells from a patient deficient in TPO signaling. These findings demonstrate a previously unrecognized function of an aaRS which may have implications for therapeutic interventions.

Author contributions: T.K., M.-N.V., S.K., R.B., X.-L.Y., Z.M.R., and P.S. designed research; T.K., M.-N.V., S.K., A.Z., R.S., Y.M., A.Y., and M.-H.D. performed research; K.E. contributed new reagents/analytic tools; T.K. and Z.M.R. analyzed data; and T.K., S.K., Z.M.R., and P.S. wrote the paper.

Reviewers: M.I., Ohio State University; and A.W., The University of Utah.

Conflict of interest statement: R.B., M.-H.D., X.-L.Y., and P.S. have a financial interest in aTyr Pharma, although none specifically for this work.

[1]T.K., M.-N.V., and S.K. contributed equally to this work.

[2]Present address: Lumos Pharma, Austin, TX 78756.

[3]To whom correspondence may be addressed. Email: ruggeri@scripps.edu or schimmel@scripps.edu.

This article contains supporting information online at www.pnas.org/lookup/suppl/doi:10.1073/pnas.1807000115/-/DCSupplemental.

Published online August 13, 2018.

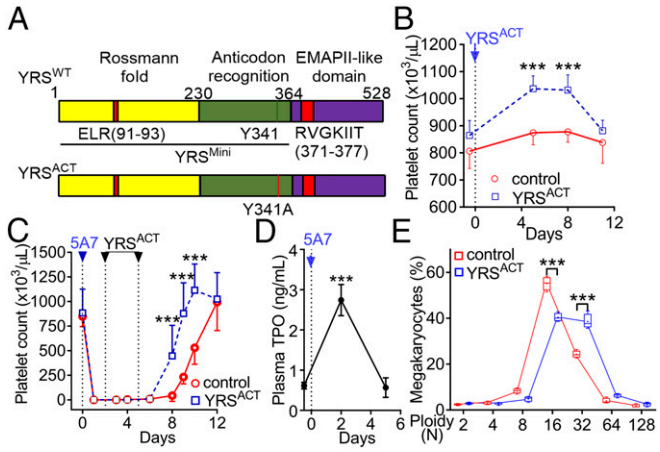

Fig. 1. YRS^{ACT} promotes platelet production in vivo. (*A*) Schematic representation of YRS domains. A Rossmann fold catalytic domain and anticodon-recognition domain, both essential for $tRNA^{Tyr}$ aminoacylation, constitute YRS^{Mini}. YRS^{ACT} contains a gain-of-function mutation (Y341A) in the context of full-length YRS. (*B*) A single injection of YRS^{ACT} (30 mg/kg), compared with vehicle (PBS), increased the blood platelet count of WT mice (n =14 in each group). (*C*) WT mice received one i.v. injection of anti-GPIbα monoclonal antibody (5A7; day 0) to deplete platelets. YRS^{ACT} (30 mg/kg) or vehicle (PBS) was injected on days 2 and 5 (n = 4) and blood cell counts were monitored at the indicated times. (*D*) Plasma samples were collected before and after (day 2) 5A7 injection, and TPO levels were determined by ELISA (n = 12). (*E*) BM cells of WT mice (n = 4) injected with YRS^{ACT} or vehicle (PBS) were harvested on day 3 and analyzed for MK ploidy by flow cytometry. Data are shown as mean ± 95% confidence interval (CI) (*B*–*D*) or 25th to 75th percentile bars with median and min to max whiskers (*E*); in the latter panel, color-coded lines join the mean values (marked by a cross indicated inside each bar) of each ploidy distribution. ***$P < 0.001$ determined by one-way ANOVA with Dunn's multiple comparison test (*D*) or two-way ANOVA with Sidak's multiple comparison test (*B*, *C*, and *E*).

were obtained and critical elements needed for activities were mapped onto each (20, 22). Breaking the tether in a rationally designed gain-of-function mutation (Y341A) converts full-length YRS into a constitutive active cytokine that, in human cell-based assays, recapitulates the activities of the two fragments (YRS^{ACT}) (23). This form allowed experiments that obviated the need to administer mixtures of fragments—a limitation that, among other considerations, severely inhibited forward integration of studies into an animal.

YRS circulates in human plasma and, unlike other tRNA synthetases, is abundantly present in platelets (24), in which protein synthesis may not be as active as nucleated cells (25). This suggested that YRS may have ex-translational roles associated with platelet biology, and prompted us to search for such possible functions. In looking at data from the cell-based assays of earlier work (18, 26), we noted that YRS^{ACT} might bind to monocytes and stimulate release of cytokines that could promote megakaryocyte expansion. We thus thought YRS may have a role in platelet biogenesis which was worth investigating in vivo. This decision was also motivated by a desire to find a link of YRS to platelet biology that could be of therapeutic relevance. Our results suggest YRS indeed has potential for offering alternative or additional treatments for thrombocytopenia and for replenishment of hematopoietic cells in a variety of applications.

Results

YRS^{ACT} Promotes Platelet Production in Vivo. To explore YRS effects on extracellular activities, we injected the constitutively active YRS^{ACT} mutant (Fig. 1*A*) or vehicle control into C57BL/6 wild-type (WT) mice. A single dose significantly increased the platelet count over a 12-d period (Fig. 1*B*); two doses accelerated the recovery from severe thrombocytopenia induced by an anti-glycoprotein (GP) Ibα antibody (Fig. 1*C*). Plasma thrombopoietin (TPO) levels peaked at day 2 post thrombocytopenia induction and returned to baseline by day 5, before platelet recovery started (Fig. 1*D*). Thus, YRS^{ACT} effect on platelet production was concurrent with maximal TPO up-regulation. Notably, there were more 32N megakaryocytes (MKs) in the bone marrow (BM) of YRS^{ACT}-treated than control mice (Fig. 1*E*), suggesting a mechanism of action of YRS^{ACT} on MKs. Moreover, YRS^{ACT}, compared with vehicle control, administered 8 and 48 h post irradiation to mice that had absorbed 300 cGy of γ-irradiation, limited the severity of thrombocytopenia and accelerated platelet count recovery (*SI Appendix*, Fig. S1). Thus, the thrombopoietic function of YRS^{ACT} could be part of a general response to thrombocytopenia.

YRS^{ACT} Enhances ex Vivo MK Expansion Independent of TPO Signaling. In agreement with in vivo results, culturing WT mouse BM cells in the presence of YRS^{ACT} for 3 d significantly stimulated MK expansion and maturation (Fig. 2 *A* and *B*). To evaluate whether this effect required TPO signaling through the c-mpl receptor (27), we compared cultures of BM cells from WT and c-$mpl^{-/-}$ mice. Although the latter contained fewer MKs, as expected, YRS^{ACT} caused a significant increase of c-$mpl^{-/-}$ MKs and shift to higher ploidy, as seen with WT MKs (Fig. 2 *A* and *B*). Furthermore, YRS^{ACT} and TPO added in combination to cultured WT BM cells yielded significantly more MKs than either alone (Fig. 2*C*), particularly with ploidy ≥32N (Fig. 2*D*). Collectively, these observations indicate that YRS^{ACT} and TPO influence MK expansion and maturation through distinct and complementary mechanisms. As a final control, we verified that YRS^{WT} (23) had no effect on MK expansion (Fig. 2 *E* and *F*), confirming that activation is essential for YRS^{ACT} function. Since YRS^{WT} and YRS^{ACT} were expressed in *Escherichia coli* and purified with an identical procedure, these results also rule out the possibility of a confounding influence of endotoxin contamination on the described effects of YRS^{ACT} on MKs.

Naturally Occurring YRS Splicing Variant Has a Biological Activity Similar to YRS^{ACT}. Subsequent to the initiation of this work, natural splice variants of YRS were identified in different human tissues and cells (5). One of these variants ($YRS^{SV\text{-}N13}$; *SI Appendix*, Fig. S2*A*), reported to be expressed in leukocyte, lung, and spleen, originates from an exon-skipping event that links two YRS segments in a way that should liberate critical elements in each and thereby mimic YRS^{ACT} (5). We expressed and purified this natural YRS variant and found that, similar to YRS^{ACT}, it increased the number of MKs in mouse BM cell cultures, particularly those with higher ploidy (*SI Appendix*, Fig. S2*B*). The biological role of a naturally occurring variant such as $YRS^{SV\text{-}N13}$ as opposed to proteolysis-derived YRS^{ACT} is a topic of future interest.

MKs Induced by YRS^{ACT} in Culture Contain a Unique Sca-1^+F4/80^+ Population. Addition of YRS^{ACT} to mouse BM cell cultures markedly increased the number of adherent cells. Among these, or in close proximity to adherent cells, we identified a population of large cells that expressed the specific MK marker GPIbα but, unexpectedly, also the stem cell marker Sca-1 and the monocyte/macrophage marker F4/80 (Fig. 3*A*). Notably, there was no expansion of Sca-1^+F4/80^+ MKs in BM cell cultures treated with TPO or IL-6 instead of YRS^{ACT} (Fig. 3*B*), indicating that expanding this MK population is not a common property of agents stimulating platelet production. Sca-1 is a recognized stem cell marker that is not normally expressed by differentiated cells such as MKs (28). Indeed, freshly isolated WT mouse BM cells contained only a small proportion (4.5 ± 0.6%, n = 4) of mature polyploid MKs gated on CD41 expression, and that on forward scatter (FSC) were also positive for Sca-1 and F4/80 (Fig. 3 *C* and *D*). The kinetics of Sca-1^+F4/80^+ MK induction

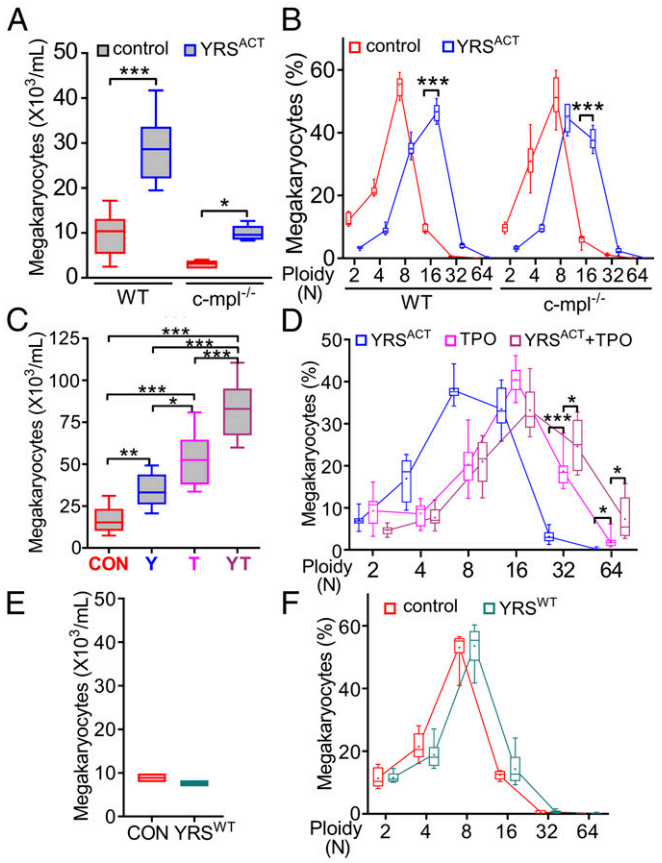

Fig. 2. YRS^{ACT} induces ex vivo MK expansion independent of TPO signaling. (*A*) BM cells isolated from WT or c-mpl$^{-/-}$ mice ($n = 6$) were cultured for 3 d with PBS or 100 nM YRS^{ACT} and analyzed for MK number. (*B*) The cultures were analyzed for MK ploidy. Data are shown as 25th to 75th percentile bars with median and min to max whiskers. (*C*) BM cells isolated from WT mice ($n = 12$) were treated with 100 nM YRS^{ACT} (Y), 1.4 nM TPO (T), YRS^{ACT} plus TPO (YT), or PBS as control (CON) for 3 d; MKs were then counted. (*D*) Selected culture conditions described in *C* were analyzed for ploidy distribution. Data are shown as in *A* and *B*. $*P < 0.05$, $**P < 0.01$, $***P < 0.001$ determined by one-way ANOVA followed by Sidak's multiple comparison test (*A*) or Tukey's multiple comparison test (*C*), or two-way ANOVA with Sidak's multiple comparison test (*B* and *D*). (*E*) Pooled BM cells from two WT mice were cultured with added YRS^{WT} (100 nM) or PBS (CON) for 3 d; MKs were then counted. (*F*) The cultures described in *E* were analyzed for ploidy distribution. Data of two experiments with technical triplicates are shown as min to max floating bars with mean. In *B* and *F*, color-coded lines join the mean values (marked by a cross indicated inside each bar) of each ploidy distribution.

was tested in WT mouse BM cell cultures monitored daily for 3 d after addition of YRS^{ACT}. The relative increase of Sca-1$^+$F4/80$^+$ MKs was progressive in the first 2 d and changed only marginally on day 3 (Fig. 3*E*). On the latter day, a comparison of Sca-1– and F4/80-positive or negative MKs (Fig. 3 *F* and *G*) showed that the positive ones had a higher FSC indicative of advanced maturation (Fig. 3*H*).

YRS^{ACT} Administration Stimulates the Expansion of Sca-1$^+$F4/80$^+$ MKs in the BM in Vivo. To test whether Sca-1$^+$F4/80$^+$ MK expansion occurs in vivo as well as in BM cell cultures, we injected two YRS^{ACT} doses, or vehicle control, into mice rendered thrombocytopenic by anti-GPIbα antibody treatment and then monitored the platelet count (Fig. 4*A*). In BM cells harvested 2 d after the last YRS^{ACT} dose, the percentage of Sca-1$^+$F4/80$^+$ MKs was significantly higher in treated than control mice (Fig. 4*B*). In agreement with in vitro results, Sca-1$^+$F4/80$^+$ MKs with 32N ploidy were significantly more numerous in YRS^{ACT}-treated than in control mice (Fig. 4*C*), while the ploidy distribution of Sca-1$^-$F4/80$^-$ MKs was not changed by YRS^{ACT} treatment (Fig. 4*D*). Thus, YRS^{ACT} selectively expands a distinct MK population. Increase of this distinct MK population in the BM coincides with the timing of YRS^{ACT}-induced platelet count recovery from thrombocytopenia, suggesting that Sca-1$^+$F4/80$^+$ MKs may be crucial for rapid platelet replenishment in extreme conditions.

YRS^{ACT} Targets Monocytic Cells to Mediate MK Expansion. Induction of Sca-1$^+$F4/80$^+$ MKs is a distinct effect of YRS^{ACT}, but because enhanced platelet production involves also Sca-1$^-$F4/80$^-$ MKs,

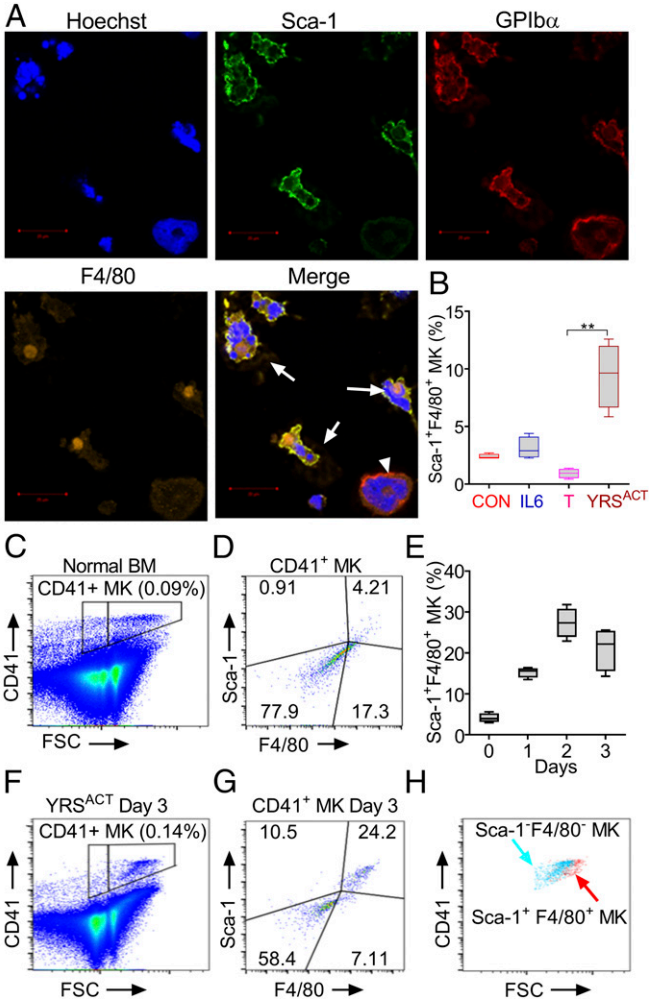

Fig. 3. Unique MK population expressing Sca-1 and F4/80 is induced by YRS^{ACT} in mouse BM cells cultured in vitro. (*A*) BM cells isolated from human GPIbα transgenic mice (mGPIbα^{null};hGPIbα^{Tg}) and cultured in the presence of 100 nM YRS^{ACT} for 3 d were analyzed by immunofluorescent staining and confocal microscopy. MKs were identified by staining with anti-hGPIbα antibody (LJ-1b1). Arrows indicate Sca-1$^+$F4/80$^+$ MKs; the arrowhead indicates a Sca-1$^-$F4/80$^-$ MK. (*B*) WT mouse BM cells ($n = 4$) were treated with 2.3 nM IL-6 (IL6), 1.4 nM TPO (T), 100 nM YRS^{ACT}, or PBS as control (CON) for 3 d and analyzed by flow cytometry. $**P < 0.01$ determined by one-way ANOVA with Dunn's multiple comparison test. (*C*) BM cells freshly isolated from a WT mouse were gated for MKs based on CD41 binding and FSC. (*D*) MKs gated in *C* analyzed for Sca-1 and F4/80 expression. (*E*) Time course of Sca-1$^+$F4/80$^+$ MK expansion (%) after YRS^{ACT} addition to BM cell cultures. (*F*) WT mouse BM cells treated with 100 nM YRS^{ACT} for 3 d were gated for MKs as in *C*. (*G*) MKs gated in *F* analyzed for Sca-1 and F4/80 expression. (*H*) Sca-1$^-$F4/80$^-$ and Sca-1$^+$F4/80$^+$ MKs identified in *G* were backgated for CD41 expression and size (FSC) showing that Sca-1$^+$F4/80$^+$ MKs are larger than Sca-1$^-$F4/80$^-$ MKs.

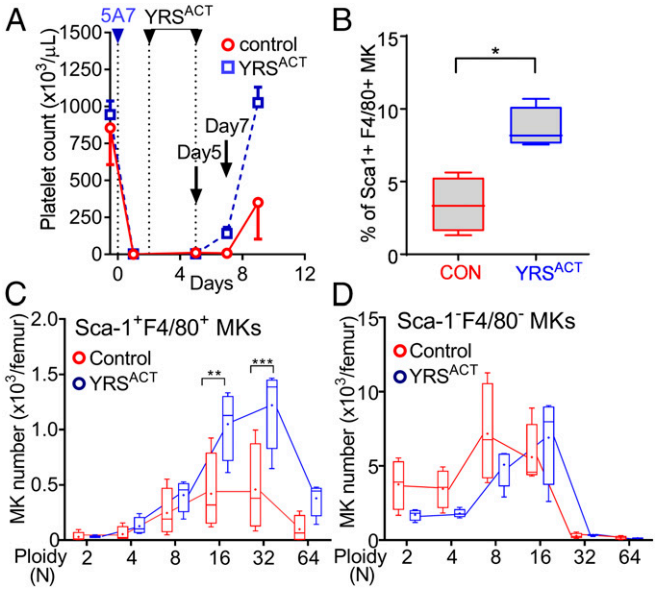

Fig. 4. Induction of Sca-1$^+$F4/80$^+$ MKs and platelets by YRS^{ACT} administration into thrombocytopenic mice. (*A*) Acute thrombocytopenia induction (day 0) and YRS^{ACT} or PBS (control) administration (days 2 and 5) were as described in Fig. 1*C* ($n = 4$ in each group). Platelets were counted on days −1, 2, 5, 7, and 9. (*B–D*) BM cells were harvested from femurs on day 7 and analyzed by flow cytometry to determine the percentage of Sca-1-F4/80–positive and –negative MKs (*B*) and respective ploidy distribution (*C* and *D*). Data are shown as mean ± 95% CI (*A*) or 25th to 75th percentile bars with median and min to max whiskers in other panels; in *C* and *D*, color-coded lines join the mean values (marked by a cross indicated inside each bar) of each ploidy distribution. $*P < 0.05$, $**P < 0.01$, $***P < 0.001$ calculated by two-tailed Mann–Whitney test (*B*) or two-way ANOVA with Sidak's multiple comparison test (*C*).

the contribution of multiple mechanisms that may include direct targeting of hematopoietic progenitors and/or other BM cells is suggested. We evaluated the effect of YRS^{ACT} using expandable CD41$^+$ hematopoietic progenitors generated by transducing WT mouse BM cells with the LIM-homeobox 2 gene (Lhx2). This method has been used to generate myeloid, erythroid, and MK lineages from BM cells or hematopoietic progenitor cells derived from embryonic or induced pluripotent stem cells (ESCs/iPSCs) (29, 30). CD41 (integrin αIIb) is expressed on MKs, but also on myeloid-biased long-term hematopoietic stem cells (HSCs) that develop in vitro and in vivo into committed MK progenitors and mature MKs (31, 32). In culture, 30 to 60% of Lhx2-transduced CD41$^+$ cells (CD41$^+$Lhx2) maintained the c-kit$^+$, Sca-1$^+$, Lin$^-$ (KSL) phenotype and also produced high-ploidy MKs (Fig. 5 *A* and *B*). Direct treatment of CD41$^+$Lhx2 cells with YRS^{ACT} failed to influence MK expansion; in contrast, supernatant from YRS^{ACT}-treated human peripheral blood mononuclear cell (hPBMC) cultures increased significantly not only the number of MKs but also the proportion of those with ploidy 16N and 32N (Fig. 5*C*). These findings indicate that one or more distinct cell lineages present in BM cultures likely mediate MK expansion by YRS^{ACT}.

To test this hypothesis further, we measured 59 cytokines in culture supernatants of WT BM cells treated or not with YRS^{ACT} and identified 11 that increased more than twofold (*SI Appendix*, Table S1). These included IL-6, IL-1α, and VEGF-A, all known to stimulate megakaryopoiesis and/or thrombopoiesis (33–36). To test whether monocytes/macrophages, which support stress-induced erythroblast proliferation and survival (37, 38), also mediate YRS^{ACT} effects on megakaryopoiesis, we injected YRS^{ACT} into WT mice previously treated with clodronate-encapsulated liposomes to deplete macrophages or PBS-encapsulated liposomes as control (39). Total BM cell numbers were not different in the two groups (Fig. 5*D*, *Left*), but clodronate-treated mice had fewer MKs and fewer TER119$^+$ erythrocytes than controls (Fig. 5*D*, *Middle* and *Right*), consistent with macrophages mediating YRS^{ACT}-induced MK expansion and maturation.

Thrombopoietic Activity of YRS^{ACT} Is Relevant in Human Cells. To establish that YRS^{ACT} influences human as well as mouse megakaryopoiesis, we used peripheral blood-derived CD34$^+$ cells from G-CSF–treated donors (40). As with mouse CD41$^+$Lhx2 cells, direct YRS^{ACT} stimulation failed to boost MK development; in

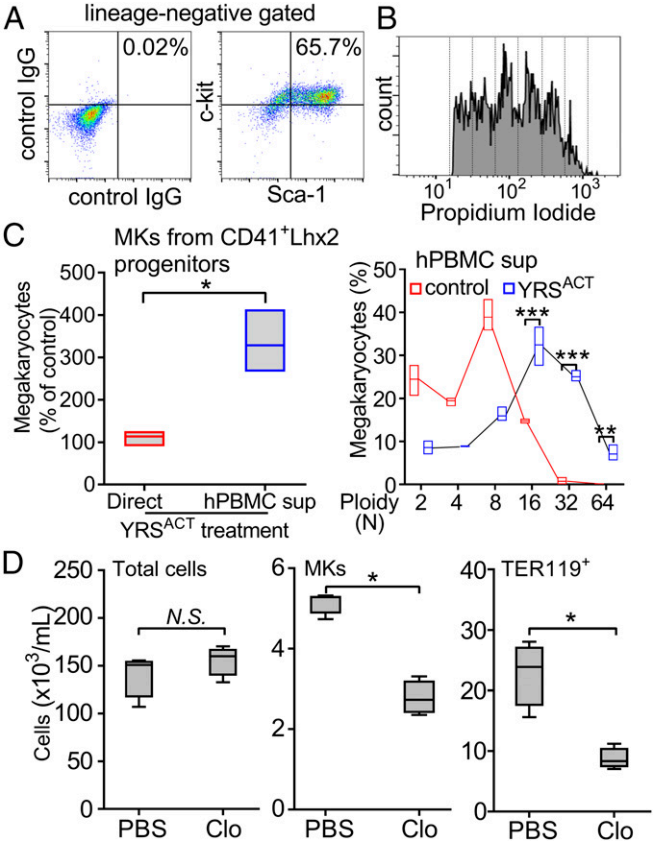

Fig. 5. Monocytes/macrophages targeted by YRS^{ACT} mediate effects on MKs. (*A* and *B*) CD41$^+$ cells isolated from WT mouse BM were transduced with the Lhx2 retrovirus for in vitro expansion. CD41$^+$Lhx2 cells were cultured in the presence of stem cell factor (SCF), TPO, and IL-6, and analyzed by flow cytometry for KSL cell expansion and megakaryocyte ploidy. (*C*, *Left*) CD41$^+$Lhx2 cells were cultured with added 100 nM YRS^{ACT} or PBS control (Direct; $n = 3$, in triplicate) or human peripheral blood mononuclear cells derived from healthy donors ($n = 3$) were cultured for 2 d with added 100 nM YRS^{ACT} or PBS, after which culture supernatants were transferred to CD41$^+$Lhx2 cells (hPBMC sup). After 3 d in culture, CD41$^+$Lhx2 cells were harvested and analyzed. MK counts in cultures exposed to YRS^{ACT} are expressed as the percent of those in PBS-treated control cultures and shown as min to max floating bars with mean. $*P < 0.05$ determined by two-tailed Welch's *t* test. (*C*, *Right*) Analysis of MK ploidy distribution in cultures exposed to hPBMC supernatants; color-coded lines join the mean values of each ploidy distribution. $**P < 0.01$, $***P < 0.001$ determined by two-way ANOVA with Sidak's multiple comparison test. (*D*) Clodronate (Clo)- or PBS-encapsulated liposomes were injected into WT mice ($n = 4$) on day 0, and then YRS^{ACT} was given i.v. on days 1 and 3; BM cells were harvested for MK count on day 4. Clodronate liposomes had no effect on total BM cell number (*Left*) but reduced MKs (*Middle*) and TER119$^+$ erythrocytes (*Right*). Data are shown as 25th to 75th percentile bars with median and min to max whiskers. $*P < 0.05$ calculated by two-tailed Mann–Whitney test. *N.S.*, not significant.

contrast, adding culture supernatant of YRS^{ACT}-treated hPBMCs increased the number of CD41^{+} MKs (Fig. 6*A*). Likewise, iPS-derived human CD34^{+} cells (41) failed to respond directly to YRS^{ACT}, but MK expansion was seen after exposure to YRS^{ACT}-treated hPBMC culture supernatant (Fig. 6*B*). We also tested iPS-derived CD34^{+} cells generated from a patient with congenital amegakaryocytic thrombocytopenia (CAMT) (42). In this condition, MK expansion and differentiation are severely impaired as a consequence of mutations in the c-mpl gene (43) causing a defective response to TPO stimulation. As with the normal counterpart, iPS-derived CD34^{+} cells from a CAMT patient failed to respond to YRS^{ACT} directly, but did so when exposed to YRS^{ACT}-treated hPBMC culture supernatant (Fig. 6*C*). Altogether, these findings show that YRS^{ACT} supports mouse and human MK expansion and maturation by stimulating monocyte/macrophage cytokine production independent of TPO signaling.

IL-6 Plays a Pivotal Role in Mediating the Effect of YRS^{ACT}. Among the monokines up-regulated by YRS^{ACT}, IL-6—known to enhance thrombopoiesis in vivo (33, 34)—increased dose-dependently in YRS^{ACT}-treated culture supernatants of monocytic THP-1 cells and hPBMCs, but not of T-cell lymphoblast-like Jurkat cells (*SI Appendix*, Fig. S3 *A* and *B*). In culture supernatants of mouse BM cells exposed to different YRS^{ACT} doses, IL-6 levels increased in parallel with MK and F4/80^{+} monocyte/macrophage numbers (Fig. 7*A*). VEGF-A and IL-1α also increased in response to YRS^{ACT}, but relatively less than IL-6, with peak levels in culture supernatants not exceeding 50 and 5 pg/mL, respectively (*SI Appendix*, Fig. S3*C*). When WT mouse BM cells were treated with YRS^{ACT} in the presence of anti–IL-6R–blocking antibodies, MK expansion was attenuated (*SI Appendix*, Fig. S4). Of note, addition of YRS^{ACT} to cultures of BM cells from IL-6$^{-/-}$ mice failed to influence MK expansion, while the percentage of Sca-1^{+}F4/80^{+} MKs was significantly higher than in untreated IL-6$^{-/-}$ BM cell cultures (Fig. 7*B*). These results indicate that induction of Sca-1^{+}F4/80^{+} MKs and enhancement of megakaryopoiesis through up-regulation of monocyte/macrophage IL-6 secretion are independent and separate YRS^{ACT} functions.

The Effect of YRS^{ACT} Is Dependent on the Toll-Like Receptor/MyD88 Signaling Pathway. We noted that many cytokines secreted by YRS^{ACT}-treated monocytic cells are regulated by NF-κB (44) activated through Toll-like receptor (TLR)-initiated MyD88 signaling (45). This observation—and the previous one that Pam3CSK4, a TLR2 ligand, promotes MK maturation (46)—suggested that YRS^{ACT} binding to TLR2 on monocytic cells activates the MyD88/NF-κB pathway to boost cytokine production. Accordingly, YRS^{ACT}-treated hPBMC lysates enhanced IKKα and IκB phosphorylation (Fig. 7*C*); this is known to be followed by phosphorylated IκB degradation promoting NF-κB nuclear translocation with expression of inflammatory cytokines (45). Moreover, megakaryopoiesis was not enhanced (Fig. 7*D*) following YRS^{ACT} stimulation of BM cells from mice lacking MyD88—the adaptor for signaling downstream of all TLRs except TLR3 (47)—and YRS^{ACT} failed to increase the platelet count of MyD88$^{-/-}$ mice (*SI Appendix*, Fig. S5). However, YRS^{ACT} treatment of TLR2$^{-/-}$ mouse BM cells enhanced megakaryopoiesis (Fig. 7*E*), suggesting the involvement of other TLRs; coprecipitation by polyclonal anti-YRS antibodies of TLR2 and TLR4 from mixtures with YRS^{ACT} (Fig. 7*F*) was in agreement with this possibility. Supporting a TLR4 role, YRS^{ACT} treatment of TLR2$^{-/-}$ BM cells in the presence of TLR4-blocking antibodies reduced MK numbers, particularly of 16N ploidy, and decreased IL-6 levels in culture supernatants (*SI Appendix*, Fig. S6 *A*–*C*). Thus, TLR2 and TLR4 may both contribute to YRS^{ACT}-induced stimulation of megakaryopoiesis.

Starting from this evidence, we investigated how activation could influence YRS function in stimulating megakaryopoiesis and found that, by coimmunoprecipitation, HEK293 cells overexpressing TLR4 bound YRS^{ACT} more robustly than YRS^{WT} (*SI Appendix*, Fig. S6*D*). This result suggests that without proteolytic cleavage, YRS^{WT} does not efficiently bind to TLRs nor influence megakaryopoiesis. In agreement with our result shown in Fig. 2*E* and also with previous work (18, 23), these results indicate that a conformational change in activated YRS contributes to the repurposing of its function by enhancing binding to one or more receptors.

Discussion

YRS^{ACT} Mediates MK-Biased Hematopoiesis Under Stress. In the condition of homeostasis, MKs are thought to arise from a common MK/erythroid progenitor (48). More recently, alternative pathways originating from MK-biased or MK-primed HSCs that bypass intermediate commitment stages have emerged (49). These direct pathways to megakaryopoiesis are gaining consideration for their relevance to platelet production in nonhomeostatic stress situations (50). For example, stem-like megakaryocyte-committed progenitors (SL-MKPs) have been identified as an emergency machinery to produce platelets under inflammatory stress (51). Here we demonstrate previously unrecognized ex-translational activities of YRS^{ACT} that delineate a pathway to megakaryopoiesis based on two functions: (*i*) inducing a distinct subset of MKs; and (*ii*) up-regulating secretion of monokines, including IL-6, that support MK expansion and, ultimately, platelet production (Fig. 8).

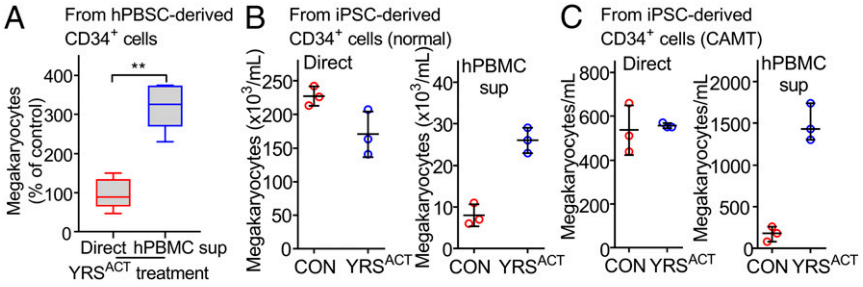

Fig. 6. Thrombopoietic activity of YRS^{ACT} is relevant in human cells. (*A*) Human CD34^{+} cells (from two donors) isolated from cryopreserved PBSCs were expanded and kept for 7 d in cultures supplemented with 200 nM YRS^{ACT} or PBS (CON), or with the supernatant of hPBMC cultures (from three donors) pretreated with YRS^{ACT} or PBS (CON) for 2 d. The number of MKs in cultures exposed to YRS^{ACT} directly (red boxes) or indirectly (blue boxes) was calculated as the percent of that in PBS-treated cultures. All hPBMC supernatants were tested in triplicate and the corresponding results were averaged for analysis. Data are shown as 25th to 75th percentile bars with median and min to max whiskers. $^{**}P < 0.01$ calculated by two-tailed Mann–Whitney test. (*B*) CD34^{+} cells from normal human iPS sacs (sac-like structures that enclose hematopoietic progenitor cells) were cultured for 14 d and then differentiated for 9 d with added YRS^{ACT} (200 nM) or PBS (*Left*), or culture supernatant of hPBMCs exposed to YRS^{ACT} or PBS (*Right*). (*C*) Experiment as in *B*, except that CD34^{+} cells were isolated from iPS cells derived from a patient with CAMT. MK counts in *C* and *D* are shown as dot plots with mean ± SD of technical triplicates.

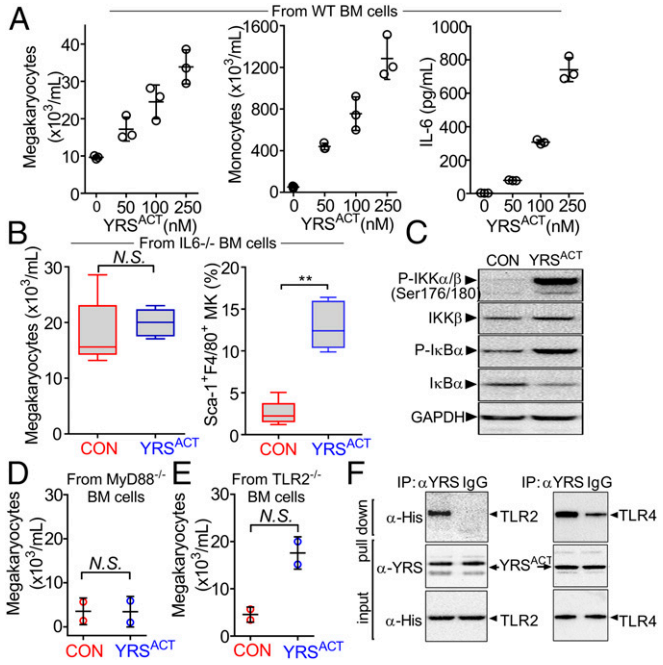

Fig. 7. Effect of YRS^{ACT} depends on the TLR/MyD88 signaling pathway. (*A*) BM cells from three WT mice were pooled and split into aliquots for treatment with different YRS^{ACT} concentrations for 3 d. Cells were analyzed for MK (*Left*) and monocyte (*Middle*) count; additionally, culture supernatants were collected to measure IL-6 by ELISA (*Right*). Each experiment was performed with technical triplicates. (*B*) BM cells from IL-6$^{-/-}$ mice ($n = 4$) were isolated and treated with YRS^{ACT} for 3 d for evaluation by flow cytometry. (*C*) Normal hPBMCs were treated with YRS^{ACT} or PBS (CON) for 20 min and then lysed and analyzed by Western blotting to evaluate NF-κB activation. (*D*) BM cells from three MyD88$^{-/-}$ mice were pooled and treated with 100 nM YRS^{ACT} or PBS (CON) for 3 d before analysis by flow cytometry ($n = 2$ with technical triplicates). (*E*) BM cells prepared from three TLR2$^{-/-}$ mice were treated with YRS^{ACT} or PBS (CON) for 3 d before analysis by flow cytometry. (*F*) YRS^{ACT} was incubated with His-tagged recombinant TLR2 or TLR4 and then mixed with anti-YRS polyclonal antibody or control IgG; the precipitate was then analyzed by immunoblotting with an anti-His tag antibody. IP, immunoprecipitation. Data are shown as dot plots with mean ± SD in *A*, *D*, and *E*, or as 25th to 75th percentile bars with median and min to max whiskers in *B*; $^*P < 0.01$ determined by Mann–Whitney two-tailed unpaired *t* test. *N.S.*, not significant.

The YRS^{ACT}-induced Sca-1$^+$F4/80$^+$ subset of MKs, identified as such by expression of platelet-specific GPIbα and large size indicating polyploidy, has not been previously characterized. The majority of these MKs, as opposed to <10% of those Sca-1$^-$F4/80$^-$, are also c-kit$^+$ (*SI Appendix*, Fig. S7). This suggests—consistent with the notion that HSCs with high c-kit expression are biased toward MK development (52)—that Sca-1$^+$F4/80$^+$ MKs originate directly from the HSC compartment. Whether they are linked to the previously reported SL-MKPs activated by stress inflammatory signals (51) remains to be investigated. We speculate that YRS secreted and activated under inflammatory stress such as viral infection may mediate the activation of SL-MKPs. The latter, however, were identified among the population of Lin$^-$cKit$^+$CD150$^+$CD48$^-$CD34$^-$ long-term HSCs, with exclusion of cells expressing leukocyte/monocyte markers. Thus, the progenitors of Sca-1$^+$F4/80$^+$ MKs may be close to but distinct from SL-MKPs; it remains to be established whether the expression of F4/80 indicates the potential of developing also into myeloid cells. YRS^{ACT}, promoting inflammatory cytokine secretion through TLR/MyD88, may stimulate Sca-1$^+$F4/80$^+$ hematopoietic progenitors in a distinct MK-biased pathway leading to rapid thrombopoiesis. Consistent with this concept, Sca-1$^+$F4/80$^+$ MKs appear in the mouse BM predominantly during the early phase of recovery from thrombocytopenia. The demonstration here that YRS^{ACT} activates TLR/MyD88 signaling and cytokine secretion in human HSCs suggests the possibility of a similar function in human diseases associated with platelet depletion. Thus, it remains to be elucidated whether YRS levels in plasma are increased in patients under inflammatory stress or with hematological disorders.

TLR/MyD88 Signaling Pathway Plays a Pivotal Role in Mediating the Effect of YRS^{ACT} on MK Expansion. We showed that interaction of YRS^{ACT} with TLR4—and possibly other TLRs—activates the TLR/MyD88/NF-κB pathway to stimulate secretion of monokines, particularly IL-6, which in turn promote MK expansion and maturation to enhance platelet production. The same TLR/MyD88 pathway activated during YRS^{ACT}-induced megakaryopoiesis is also a key player in the host innate immune defense. TLRs recognize pathogen-associated molecular patterns and are also engaged by host-derived molecules in response to tissue damage or stress (53), including heat shock proteins and high-mobility group box-1 protein (54). Like YRS^{ACT}, these ligands engage multiple TLRs, including TLR2 and TLR4. Therefore, the YRS that is secreted under stress and activated by leukocyte elastase, or a secreted active splice, may become available to stimulate TLR-based pathways, including but not limited to megakaryopoiesis (55). In addition to stress-stimulated signaling through TLR pathways, YRS translocates to the nucleus under stress and acts through its nuclear partners that include PARP-1 and TRIM28. Stress conditions that promote translocation to the nucleus include serum starvation and oxidative damage, and trigger pathways for cell rescue (9, 16, 56). Thus, the mobilization of TLR pathways by YRS for megakaryopoiesis is only one of the several roles in stress responses. Whether secreted YRS can also enter cells and the nucleus is a subject for future investigation.

Recruitment of tRNA Synthetases for Nontranslational Functions. Aminoacyl-tRNA synthetases and tRNAs arose early in evolution as determinants of the genetic code rules, and thus were available for recruitment to novel roles during development of the

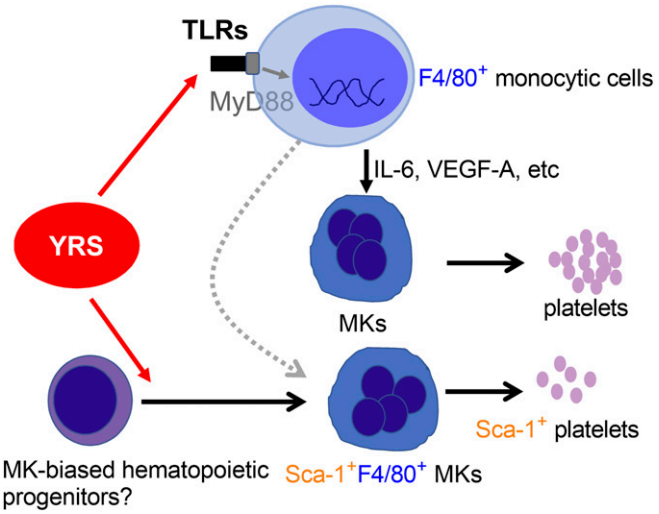

Fig. 8. Schematic representation of the mechanism of YRS^{ACT} influence on megakaryopoiesis. YRS^{ACT} targets monocytic cells and signals through the TLR/MyD88 pathway, inducing cytokine secretion that facilitates MK expansion and platelet production. One remarkable effect of YRS^{ACT} is the induction of a unique subset of MKs that express Sca-1 and F4/80 as well as MK markers. Both of these mechanisms may represent the action of YRS^{ACT} on "MK-biased hematopoiesis" that contributes to rapid MK expansion and platelet replenishment under stress conditions.

tree of life. Both became involved in signaling pathways beyond protein synthesis, and both depended on modifications secondary to splitting (or fragmentation) to repurpose themselves (1, 57–62). For tRNA synthetases, the addition of new domains correlates with progression in evolution. For example, the UNE-S domain added to seryl-tRNA synthetase correlates with the passage from the invertebrate open to the vertebrate closed circulatory system (15). UNE-S, which is dispensable for aminoacylation, harbors a nuclear localization signal (NLS) that is essential to bring SerRS into the nucleus, where it regulates VEGF-A signaling and vascular development (63). Impairing NLS function prevents nuclear import and development of the closed circulatory system, explaining the selective pressure to retain UNE-S throughout vertebrate evolution. Similarly, the ELR and EMAPII domains, needed for YRS ex-translational activities, were added at the stage of insects during evolution and then retained up to humans (64).

Interestingly, TLRs (65) and functional analogs of IL-6 (66), both important for mediating YRS^{ACT} functions, have been identified in a variety of invertebrates. In contrast, blood cells (thrombocytes) with functions similar to mammalian platelets are found only in vertebrates (67). Since these cells evolved from the hemocyte of invertebrates, the mechanisms of nontranslational YRS functions identified here may have been operating before the appearance of mammals. By linking ex-translational functions to the essential genetic code through tRNAs and tRNA synthetases, these new functions were under the highest selective pressure for retention. Exactly how this linkage occurred is unclear, but clues can be found in tryptophanyl- and tyrosyl-tRNA synthetases. In both, the amino acid-binding pocket captures either a protruding receptor side chain or a natural small ligand that matches the specificity of the pocket (16, 68). The early development of binding pockets based on the architectures of amino acid side chains created a diversity of sites that could be exploited for the recognition of amino acid side chains protruding from other protein surfaces or recapitulated in cellular ligands. Whether protruding tyrosyl side chains on proteins in the megakaryopoiesis pathway have a role in the recruitment of YRS is open to further investigation.

Implications for Management of Thrombocytopenia. Recombinant IL-6 has been considered for treatment of thrombocytopenia, but serious side effects, such as fever, fatigue, and dilution anemia, presumably caused by the frequent systemic administration needed for pharmacological activity, have limited evaluation of its efficacy (69, 70). In this regard, among other possibilities, YRS^{ACT} provides a new approach to introduce IL-6 as a therapeutic agent. We showed a single i.v. injection of YRS^{ACT} was sufficient to increase blood platelet counts. This is consistent with activation of monocytes/macrophages occurring in the BM microenvironment so that IL-6 release and pharmacological activity are localized. Accordingly, IL-6 plasma levels were minimally changed by YRS^{ACT} injection in mice (*SI Appendix*, Fig. S8). In addition, while less prominent than IL-6, we detected other cytokines (e.g., VEGF) that are released upon YRS^{ACT} administration and also are known for thrombopoietic activities (35). Thus, it remains possible that other factors are also part of the polybiology associated with YRS^{ACT}.

TPO mimetics are Food and Drug Administration-approved as a second-line treatment for idiopathic thrombocytopenia. However, their use is associated with risks that include thrombosis, BM fibrosis, and acute myelogenous leukemia (71, 72). In addition, alternative treatment options are desired for thrombocytopenic patients unresponsive to TPO mimetics, such as those affected by CAMT. Because YRS^{ACT} can stimulate megakaryocyte expansion and maturation independent of TPO signaling, it could represent a first step toward the pharmacological treatment of pathological conditions for which TPO mimetics are not effective. In addition, because of a distinct mechanism of action, YRS^{ACT} may enhance therapeutic benefits of TPO mimetics when coadministered in vivo. Currently, application of TPO mimetics is restricted due to limited efficacy in specific pathological conditions. For example, earlier studies testing recombinant TPO or TPO mimetics in patients with chemotherapy-induced thrombocytopenia did not show significant shortening of critical thrombocytopenia (73–75). For this reason, further studies of ways to optimize the treatment regimen are ongoing (76). Because YRS^{ACT} induces megakaryocyte-biased hematopoiesis and accelerates platelet recovery, it may provide benefits in combination with TPO mimetics, and thereby provide the needed path toward optimization of the treatment regimen. In addition, our demonstration of ex vivo activity suggests the possibility of YRS^{ACT} being used to boost the yield of cell culture-based methods for preparation of platelet concentrates for transfusions (77). Finally, our data demonstrate the effectiveness of YRS^{ACT} in expanding MKs in a CAMT patient, and thus strongly suggest YRS^{ACT} as a bridging supportive therapy before hematopoietic stem cell transplantation.

In summary, we have demonstrated repurposing of an aaRS for hematopoiesis and platelet biology. These results suggest that endogenous YRS, either proteolytically cleaved or expressed as activated splicing variants, plays a role in regulating megakaryopoiesis under stress conditions. The TPO-independent action of YRS^{ACT} and induction of MK-biased hematopoiesis leading to rapid thrombopoiesis suggest the therapeutic utility of YRS^{ACT} for hematological diseases.

Materials and Methods

Human Subjects. Human samples were obtained in accordance with the Helsinki Declaration after obtaining written informed consent. The experimental protocol was approved by The Scripps Research Institute (TSRI) Institutional Review Board (IRB-125923). Details of hPBMC preparation, YRS^{ACT} treatment, and culture supernatant transfer experiments to see the effect on MKs can be found in *SI Appendix, Materials and Methods*.

Animal Experiments. The experimental animals used in this study were housed in the vivarium at TSRI and approved for use by the Institutional Laboratory Animal Care and Used Committee. All animal procedures were performed in accordance with NIH *Guidelines for the Care and Use of Laboratory Animals* (78). Details of the source of each strain, in vivo experiments, BM cell culture, and MK ploidy analysis are described in *SI Appendix, Materials and Methods*.

Preparation of recombinant YRS^{ACT} protein, confocal analysis, immunoprecipitation and Western blotting, and measurement of IL-6 are described in *SI Appendix, Materials and Methods*.

ACKNOWLEDGMENTS. We thank L. De Marco and M. Mazzucato (Department of Translational Research, National Cancer Center, IRCCS CRO) for providing human peripheral blood stem cells. This work was supported by aTyr Pharma, NIH Grants HL117722 and HL135294 (to Z.M.R.), CA92577 (to P.S.), and HL129011 (to T.K.), and a fellowship from the National Foundation for Cancer Research (to P.S.). T.K. is a past recipient, and S.K. and A.Z. are current recipients, of Junior Faculty Transition Awards from the MERU Foundation, Italy.

1. Guo M, Schimmel P (2013) Essential nontranslational functions of tRNA synthetases. *Nat Chem Biol* 9:145–153.
2. Mukhopadhyay R, Jia J, Arif A, Ray PS, Fox PL (2009) The GAIT system: A gatekeeper of inflammatory gene expression. *Trends Biochem Sci* 34:324–331.
3. Mirando AC, Francklyn CS, Lounsbury KM (2014) Regulation of angiogenesis by aminoacyl-tRNA synthetases. *Int J Mol Sci* 15:23725–23748.
4. Kim S, You S, Hwang D (2011) Aminoacyl-tRNA synthetases and tumorigenesis: More than housekeeping. *Nat Rev Cancer* 11:708–718.
5. Lo WS, et al. (2014) Human tRNA synthetase catalytic nulls with diverse functions. *Science* 345:328–332.
6. Sampath P, et al. (2004) Noncanonical function of glutamyl-prolyl-tRNA synthetase: Gene-specific silencing of translation. *Cell* 119:195–208.
7. Arif A, et al. (2017) EPRS is a critical mTORC1-S6K1 effector that influences adiposity in mice. *Nature* 542:357–361.
8. Han JM, et al. (2012) Leucyl-tRNA synthetase is an intracellular leucine sensor for the mTORC1-signaling pathway. *Cell* 149:410–424.

9. Wei N, et al. (2014) Oxidative stress diverts tRNA synthetase to nucleus for protection against DNA damage. *Mol Cell* 56:323–332.
10. Takashima Y, et al. (2014) Resetting transcription factor control circuitry toward ground-state pluripotency in human. *Cell* 158:1254–1269.
11. Park MC, et al. (2012) Secreted human glycyl-tRNA synthetase implicated in defense against ERK-activated tumorigenesis. *Proc Natl Acad Sci USA* 109:E640–E647.
12. He W, et al. (2015) CMT2D neuropathy is linked to the neomorphic binding activity of glycyl-tRNA synthetase. *Nature* 526:710–714.
13. Son SH, Park MC, Kim S (2014) Extracellular activities of aminoacyl-tRNA synthetases: New mediators for cell-cell communication. *Top Curr Chem* 344:145–166.
14. Yannay-Cohen N, et al. (2009) LysRS serves as a key signaling molecule in the immune response by regulating gene expression. *Mol Cell* 34:603–611.
15. Xu X, et al. (2012) Unique domain appended to vertebrate tRNA synthetase is essential for vascular development. *Nat Commun* 3:681.
16. Sajish M, Schimmel P (2015) A human tRNA synthetase is a potent PARP1-activating effector target for resveratrol. *Nature* 519:370–373.
17. Tzima E, et al. (2005) VE-cadherin links tRNA synthetase cytokine to anti-angiogenic function. *J Biol Chem* 280:2405–2408.
18. Wakasugi K, Schimmel P (1999) Two distinct cytokines released from a human aminoacyl-tRNA synthetase. *Science* 284:147–151.
19. Wakasugi K, et al. (2002) Induction of angiogenesis by a fragment of human tyrosyl-tRNA synthetase. *J Biol Chem* 277:20124–20126.
20. Yang XL, Skene RJ, McRee DE, Schimmel P (2002) Crystal structure of a human aminoacyl-tRNA synthetase cytokine. *Proc Natl Acad Sci USA* 99:15369–15374.
21. Wakasugi K, Quinn CL, Tao N, Schimmel P (1998) Genetic code in evolution: Switching species-specific aminoacylation with a peptide transplant. *EMBO J* 17:297–305.
22. Yang X-L, Liu J, Skene RJ, McRee DE, Schimmel P (2003) Crystal structure of an EMAP-II-like cytokine released from a human tRNA synthetase. *Helv Chim Acta* 86: 1246–1257.
23. Yang XL, et al. (2007) Gain-of-function mutational activation of human tRNA synthetase procytokine. *Chem Biol* 14:1323–1333.
24. Marcus K, Immler D, Sternberger J, Meyer HE (2000) Identification of platelet proteins separated by two-dimensional gel electrophoresis and analyzed by matrix assisted laser desorption/ionization-time of flight-mass spectrometry and detection of tyrosine-phosphorylated proteins. *Electrophoresis* 21:2622–2636.
25. Weyrich AS, Schwertz H, Kraiss LW, Zimmerman GA (2009) Protein synthesis by platelets: Historical and new perspectives. *J Thromb Haemost* 7:241–246.
26. Vo MN, Yang XL, Schimmel P (2011) Dissociating quaternary structure regulates cell-signaling functions of a secreted human tRNA synthetase. *J Biol Chem* 286: 11563–11568.
27. Kuter DJ (2014) Milestones in understanding platelet production: A historical overview. *Br J Haematol* 165:248–258.
28. Holmes C, Stanford WL (2007) Concise review: Stem cell antigen-1: Expression, function, and enigma. *Stem Cells* 25:1339–1347.
29. Pinto do O P, Richter K, Carlsson L (2002) Hematopoietic progenitor/stem cells immortalized by Lhx2 generate functional hematopoietic cells in vivo. *Blood* 99: 3939–3946.
30. Kitajima K, Minehata K, Sakimura K, Nakano T, Hara T (2011) In vitro generation of HSC-like cells from murine ESCs/iPSCs by enforced expression of LIM-homeobox transcription factor Lhx2. *Blood* 117:3748–3758.
31. Gekas C, Graf T (2013) CD41 expression marks myeloid-biased adult hematopoietic stem cells and increases with age. *Blood* 121:4463–4472.
32. Nishikii H, et al. (2015) Unipotent megakaryopoietic pathway bridging hematopoietic stem cells and mature megakaryocytes. *Stem Cells* 33:2196–2207.
33. Asano S, et al. (1990) In vivo effects of recombinant human interleukin-6 in primates: Stimulated production of platelets. *Blood* 75:1602–1605.
34. Ishibashi T, et al. (1989) Interleukin-6 is a potent thrombopoietic factor in vivo in mice. *Blood* 74:1241–1244.
35. Pitchford SC, Lodie T, Rankin SM (2012) VEGFR1 stimulates a CXCR4-dependent translocation of megakaryocytes to the vascular niche, enhancing platelet production in mice. *Blood* 120:2787–2795.
36. Nishimura S, et al. (2015) IL-1α induces thrombopoiesis through megakaryocyte rupture in response to acute platelet needs. *J Cell Biol* 209:453–466.
37. Ramos P, et al. (2013) Macrophages support pathological erythropoiesis in polycythemia vera and β-thalassemia. *Nat Med* 19:437–445.
38. Chow A, et al. (2013) CD169^{+} macrophages provide a niche promoting erythropoiesis under homeostasis and stress. *Nat Med* 19:429–436.
39. Weisser SB, van Rooijen N, Sly LM (2012) Depletion and reconstitution of macrophages in mice. *J Vis Exp* (66):4105.
40. Abbruzzese L, et al. (2010) A new freezing and storage procedure improves safety and viability of haematopoietic stem cells and neutrophil engraftment: A single institution experience. *Vox Sang* 98:172–180.
41. Takayama N, Eto K (2012) In vitro generation of megakaryocytes and platelets from human embryonic stem cells and induced pluripotent stem cells. *Methods Mol Biol* 788:205–217.
42. Hirata S, et al. (2013) Congenital amegakaryocytic thrombocytopenia iPS cells exhibit defective MPL-mediated signaling. *J Clin Invest* 123:3802–3814.
43. Ballmaier M, Germeshausen M (2011) Congenital amegakaryocytic thrombocytopenia: Clinical presentation, diagnosis, and treatment. *Semin Thromb Hemost* 37: 673–681.
44. Pahl HL (1999) Activators and target genes of Rel/NF-kappaB transcription factors. *Oncogene* 18:6853–6866.
45. Kawai T, Akira S (2007) Signaling to NF-kappaB by Toll-like receptors. *Trends Mol Med* 13:460–469.
46. Beaulieu LM, Lin E, Morin KM, Tanriverdi K, Freedman JE (2011) Regulatory effects of TLR2 on megakaryocytic cell function. *Blood* 117:5963–5974.
47. Kawai T, Akira S (2006) TLR signaling. *Cell Death Differ* 13:816–825.
48. Debili N, et al. (1996) Characterization of a bipotent erythro-megakaryocytic progenitor in human bone marrow. *Blood* 88:1284–1296.
49. Sanjuan-Pla A, et al. (2013) Platelet-biased stem cells reside at the apex of the haematopoietic stem-cell hierarchy. *Nature* 502:232–236.
50. Müller-Newen G, Stope MB, Kraus T, Ziegler P (2017) Development of platelets during steady state and inflammation. *J Leukoc Biol* 101:1109–1117.
51. Haas S, et al. (2015) Inflammation-induced emergency megakaryopoiesis driven by hematopoietic stem cell-like megakaryocyte progenitors. *Cell Stem Cell* 17:422–434.
52. Shin JY, Hu W, Naramura M, Park CY (2014) High c-Kit expression identifies hematopoietic stem cells with impaired self-renewal and megakaryocytic bias. *J Exp Med* 211:217–231.
53. Erridge C (2010) Endogenous ligands of TLR2 and TLR4: Agonists or assistants? *J Leukoc Biol* 87:989–999.
54. Piccinini AM, Midwood KS (2010) DAMPening inflammation by modulating TLR signalling. *Mediators Inflamm* 2010:672395.
55. Nagai Y, et al. (2006) Toll-like receptors on hematopoietic progenitor cells stimulate innate immune system replenishment. *Immunity* 24:801–812.
56. Fu G, Xu T, Shi Y, Wei N, Yang XL (2012) tRNA-controlled nuclear import of a human tRNA synthetase. *J Biol Chem* 287:9330–9334.
57. Schimmel P (2018) The emerging complexity of the tRNA world: Mammalian tRNAs beyond protein synthesis. *Nat Rev Mol Cell Biol* 19:45–58.
58. Chen Q, Yan W, Duan E (2016) Epigenetic inheritance of acquired traits through sperm RNAs and sperm RNA modifications. *Nat Rev Genet* 17:733–743.
59. Kirchner S, Ignatova Z (2015) Emerging roles of tRNA in adaptive translation, signalling dynamics and disease. *Nat Rev Genet* 16:98–112.
60. Torres AG, Batlle E, Ribas de Pouplana L (2014) Role of tRNA modifications in human diseases. *Trends Mol Med* 20:306–314.
61. Yao P, Poruri K, Martinis SA, Fox PL (2014) Non-catalytic regulation of gene expression by aminoacyl-tRNA synthetases. *Top Curr Chem* 344:167–187.
62. Motzik A, Nechushtan H, Foo SY, Razin E (2013) Non-canonical roles of lysyl-tRNA synthetase in health and disease. *Trends Mol Med* 19:726–731.
63. Shi Y, et al. (2014) tRNA synthetase counteracts c-Myc to develop functional vasculature. *eLife* 3:e02349.
64. Guo M, Yang XL, Schimmel P (2010) New functions of aminoacyl-tRNA synthetases beyond translation. *Nat Rev Mol Cell Biol* 11:668–674.
65. Buchmann K (2014) Evolution of innate immunity: Clues from invertebrates via fish to mammals. *Front Immunol* 5:459.
66. Beck G, Habicht GS (1996) Characterization of an IL-6-like molecule from an echinoderm (*Asterias forbesi*). *Cytokine* 8:507–512.
67. Weyrich AS, Lindemann S, Zimmerman GA (2003) The evolving role of platelets in inflammation. *J Thromb Haemost* 1:1897–1905.
68. Zhou Q, et al. (2010) Orthogonal use of a human tRNA synthetase active site to achieve multifunctionality. *Nat Struct Mol Biol* 17:57–61.
69. Gordon MS, et al. (1995) A phase I trial of recombinant human interleukin-6 in patients with myelodysplastic syndromes and thrombocytopenia. *Blood* 85:3066–3076.
70. Aquino VM, Mustafa MM, Vaickus L, Wooley R, Buchanan GR (1998) Recombinant interleukin-6 in the treatment of congenital thrombocytopenia associated with absent radii. *J Pediatr Hematol Oncol* 20:474–476.
71. Gernsheimer TB (2008) The pathophysiology of ITP revisited: Ineffective thrombopoiesis and the emerging role of thrombopoietin receptor agonists in the management of chronic immune thrombocytopenic purpura. *Hematology (Am Soc Hematol Educ Program)* 2008:219–226.
72. Oshima Y, Yuji K, Tanimoto T, Hinomura Y, Tojo A (2013) Association between acute myelogenous leukemia and thrombopoietin receptor agonists in patients with immune thrombocytopenia. *Intern Med* 52:2193–2201.
73. Schiffer CA, et al. (2000) A double-blind, placebo-controlled trial of pegylated recombinant human megakaryocyte growth and development factor as an adjunct to induction and consolidation therapy for patients with acute myeloid leukemia. *Blood* 95:2530–2535.
74. Archimbaud E, et al. (1999) A randomized, double-blind, placebo-controlled study with pegylated recombinant human megakaryocyte growth and development factor (PEG-rHuMGDF) as an adjunct to chemotherapy for adults with de novo acute myeloid leukemia. *Blood* 94:3694–3701.
75. Kellum A, et al. (2010) A randomized, double-blind, placebo-controlled, dose ranging study to assess the efficacy and safety of eltrombopag in patients receiving carboplatin/paclitaxel for advanced solid tumors. *Curr Med Res Opin* 26:2339–2346.
76. Rodeghiero F, Carli G (2017) Beyond immune thrombocytopenia: The evolving role of thrombopoietin receptor agonists. *Ann Hematol* 96:1421–1434.
77. Sim X, Poncz M, Gadue P, French DL (2016) Understanding platelet generation from megakaryocytes: Implications for in vitro-derived platelets. *Blood* 127:1227–1233.
78. National Research Council (2011) *Guide for the Care and Use of Laboratory Animals* (Natl Acad Press, Washington, DC), 8th Ed.